buildings

MDPI

Article

Early-Stage Thermal Risk Diagnosis in High-Altitude Andean Residential Buildings: An Exploratory Envelope-Based Alert Matrix and Post-Simulation Discomfort Ratio

Ramiro Correa-Jaramillo * and Mercedes Torres-Gutiérrez

Departamento de Ingeniería Civil, Arquitectura y Geociencias, Universidad Técnica Particular de Loja (UTPL), San Cayetano Alto s/n, Loja 11-01-608, Ecuador
* Correspondence: racorrea@utpl.edu.ec

Abstract

High-altitude Andean climates present dual thermal pressure: daytime overheating risk coexists with nighttime heat loss within the same annual cycle. Aggregate energy indicators do not reveal the direction of thermal discomfort, limiting their utility for early-stage passive design. This study proposes a two-stage exploratory diagnostic framework for residential buildings in this context. Stage 1 uses window-to-wall ratio (WWR) and average opaque wall thermal transmittance (U-wall) to construct a preliminary thermal-risk alert matrix that is applicable at the schematic design phase. Stage 2 uses the post-simulation Discomfort Ratio (DR = Href/Hcal) to confirm the direction of thermal discomfort as overheating-dominant, heat-loss-dominant, or mixed. The framework was applied to 14 anonymized residential building energy simulation cases in Loja, Ecuador. Of 13 classifiable cases, DR assigned 5 to overheating-dominant, 5 to heat-loss-dominant, and 3 to mixed patterns; 6 cases with complete WWR and U-wall data populated the Stage 1 matrix. The surface-to-volume ratio and air changes per hour did not clearly discriminate across patterns. The framework is exploratory and corpus-specific; the alert matrix does not replace dynamic simulation and requires validation before normative or predictive application. Alongside DR, a bounded directional-intensity index (Normalized Discomfort Balance) and the total discomfort load are reported so that the direction and the magnitude of discomfort can be read jointly.

Keywords: thermal comfort; building performance simulation; building energy simulation; residential buildings; building envelope; window-to-wall ratio; thermal transmittance; Discomfort Ratio; high-altitude Andean climate; passive design

Check for updates

Academic Editor: Francesca Cappelletti

Received: 3 May 2026
Revised: 3 June 2026
Accepted: 19 June 2026
Published: 28 June 2026

Copyright: © 2026 by the authors. Licensee MDPI, Basel, Switzerland. This article is an open access article distributed under the terms and conditions of the Creative Commons Attribution (CC BY) license.

1. Introduction

Thermal comfort and energy efficiency are among the most extensively studied—and most tightly coupled—dimensions of residential building performance. Buildings that cannot maintain acceptable indoor conditions without mechanical conditioning not only incur disproportionate energy loads, but also compromise occupant health and well-being [1,2]. In the residential sector, which is the dominant source of building-related energy use in most low- and middle-income countries [3], the envelope is central to both comfort and energy demand because it mediates all heat exchange between the interior and the outdoor environment [4,5].

The relationship between building form and thermal performance has been studied extensively through building energy simulation (BES), with particular attention being paid

to geometric descriptors such as the surface-to-volume (S/V) ratio and the compactness index [6,7]. In heating-dominated temperate climates, compact forms—those with low S/V values—are associated with reduced heat loss and lower heating demand [8,9]. These associations, however, were developed largely for climates with a single dominant thermal driver, and their transferability to climates in which overheating and heat-loss risks coexist throughout the year remains underexplored [10].

High-altitude temperate Andean climates, such as those of the inter-Andean valleys of Ecuador between 2000 and 2800 m above sea level, present a combination of conditions that distinguishes them from both low-altitude tropical climates and mid-latitude temperate zones: moderate mean annual temperatures in the range of 15–18 °C, daily thermal amplitudes of 8–12 °C, persistent relative humidity between 70 and 90%, and a solar radiation profile in which partial cloud cover frequently limits passive gains [11,12]. Buildings in these climates are subject to dual thermal pressure: overheating risk during sunny daytime periods coexists with heat-loss risk during cold nights and overcast periods within the same annual cycle. This creates a design challenge that is absent in single-mode climates—a passive strategy that addresses one discomfort mode may worsen the other. For instance, high opaque thermal resistance that reduces winter heat loss may simultaneously restrict summer nighttime heat dissipation, amplifying overheating under conditions of solar or internal heat accumulation [13].

The window-to-wall ratio (WWR) and the thermal transmittance of opaque walls (U-wall, $W/m^2 \cdot K$) are recognized as key envelope parameters in thermal comfort and energy efficiency research. WWR modulates solar heat gain, daylighting, and conductive exchange through the glazing [14,15], whereas U-wall governs the rate of heat exchange through opaque surfaces: a lower U-wall corresponds to lower thermal transmittance—that is, higher thermal resistance and a better-insulated opaque assembly [16,17]. In high-altitude temperate Andean climates specifically, an envelope with low opaque thermal transmittance may simultaneously reduce heat loss and restrict nighttime heat dissipation, producing overheating that persists beyond the period of daytime solar gain [4,18]. Recent building energy simulation studies confirm that glazing ratio, opaque thermal transmittance, and thermal mass interact in shaping summer overheating, so that a single envelope variable cannot be optimized in isolation [19].

The Ecuadorian Norma Ecuatoriana de la Construcción (NEC) classifies Loja as Climate Zone 3 (highland temperate) and sets prescriptive envelope requirements for energy efficiency [13]. It does not, however, address the directional classification of thermal discomfort at the level of individual envelope configurations, nor does it provide specific guidance on the joint effect of glazing ratio and opaque-wall properties in dual-pressure climates. Most published BES studies of Andean residential buildings report aggregate energy demand without characterizing the direction of thermal discomfort [10]. Recent building energy simulation studies of Andean and Ecuadorian dwellings have advanced the assessment of adaptive comfort and envelope performance in these climates—including standardized social housing across Ecuadorian climate zones [20] and passive-envelope optimization for high-altitude rural housing [21,22]—yet they continue to report aggregate comfort or energy outcomes rather than resolving the direction of thermal discomfort at the level of individual envelope configurations.

This study does not aim to demonstrate that envelope variables influence thermal comfort, which is already well established. Accordingly, the main research question of this study is specific and, in this climatic context, still largely unresolved: at the schematic-design stage, before dynamic simulation is available, can simple envelope descriptors anticipate the direction of thermal discomfort—overheating- or heat-loss-dominant—in high-altitude Andean residential buildings subject to dual thermal pressure? The gap

this question addresses is twofold. First, most building energy simulation (BES) studies of Andean housing report aggregate energy demand without resolving the direction of discomfort. Second, the morphological indicators commonly used for early screening were calibrated for single-driver climates and are not designed for directional screening in dual-pressure contexts. To address this gap, the study proposes a practice-oriented, two-stage exploratory diagnostic framework. In Stage 1, two descriptors available at the anteproyecto (schematic design) phase—WWR and U-wall—are combined in an exploratory thermal-risk alert matrix before the architect commits to full dynamic simulation. In Stage 2, after dynamic BES, the Discomfort Ratio (DR = Href/Hcal)—reported together with a bounded directional-intensity index and the total discomfort load—confirms the direction of thermal discomfort and supports the selection of heat-retention, heat-dissipation, or balanced dual-mode passive strategies. The main contribution is therefore methodological and practice-oriented rather than predictive: it links simple architectural descriptors, a preliminary thermal-risk alert, and post-simulation directional confirmation into a single sequential workflow, without prescribing normative thresholds.

2. Materials and Methods

2.1. Climate Context

Loja, Ecuador (04°00′ S, 79°12′ W; elevation approximately 2100 m a.s.l.) lies in NEC Climate Zone 3 (highland temperate), with mean annual temperatures of 15–18 °C, daily thermal amplitudes of 8–12 °C, relative humidity of 70–90%, and annual precipitation of 800–1500 mm distributed without a pronounced dry season [13]. The heating degree-day base (HDD_{18}) ranges from approximately 614 to 900 °C·day across urban microclimatic zones, while the annual cooling-hour profile reflects a persistent, mild overheating risk driven by solar radiation on clear afternoons. Hourly climate data were obtained from METEONORM 8.x-generated EnergyPlus Weather (EPW) files for Loja. Because no systematic indoor-temperature validation campaign was conducted for the analyzed cases, the simulation outputs are interpreted as comparative indicators of the direction of thermal discomfort rather than as experimentally validated predictions of absolute energy performance.

2.2. Building Dataset and Simulation Protocol

The analytical corpus comprises fourteen (14) residential BES cases developed as course-based academic projects in the undergraduate course Environmental Analysis of Buildings (Análisis Ambiental de la Edificación) during the October 2025–February 2026 term of the Architecture program at Universidad Técnica Particular de Loja (UTPL). All cases are single-family or multi-family residential buildings located in NEC Climate Zone 3 in the urban or peri-urban area of Loja. Dynamic BES was performed with EcoDesigner STAR/EnergyPlus within Archicad 26, over a full calendar year at a one-hour time step.

Operational parameters were harmonized as far as the source academic documentation allowed: occupancy schedules, internal heat gains, ventilation rates, and thermostat setpoints were standardized to NEC-HS-EE prescriptions wherever these were specified, whereas geometry, envelope assemblies, U-values, and window areas were taken from each project's own documentation and were therefore case-specific. Because the corpus was assembled from independent course projects rather than under a single unified simulation protocol, some heterogeneity in modeling assumptions remains across cases and is acknowledged as a limitation; this heterogeneity affects the absolute values of Hcal and Href and is the reason that these outputs are interpreted only as comparative indicators of discomfort direction, not as calibrated predictions of absolute performance. To limit its influence, every case underwent the same quality-control screening before inclusion: verification of the assigned NEC climate zone and EPW file, confirmation of residential use, and a

check of the simulated Hcal and Href outputs for physical plausibility—here meaning the exclusion of results internally inconsistent with the EPW climate or the modeled envelope (for example, near-null annual discomfort in both directions, or magnitudes incompatible with the Loja climate). Student identifiers associated with each case are retained in the authors' records; cases are only reported using coded identifiers (L-xx and N-xx). No personal data of occupants, students, or study participants were used; individual project documentation is retained under institutional academic confidentiality.

The initial pool comprised eighteen (18) course-based BES projects from the same term. Each was screened for climatic consistency, residential use, physical plausibility of the simulation outputs, and completeness of the key envelope variables. A case was excluded if it met any of the following criteria: (a) a climate zone other than NEC Zone 3; (b) a primary occupancy other than residential; (c) physically implausible simulation outputs; or (d) a confirmed, geographically misassigned EPW file. Four cases were excluded on these grounds, yielding the final corpus of 14 residential BES cases. Figure 1 shows the methodological workflow.

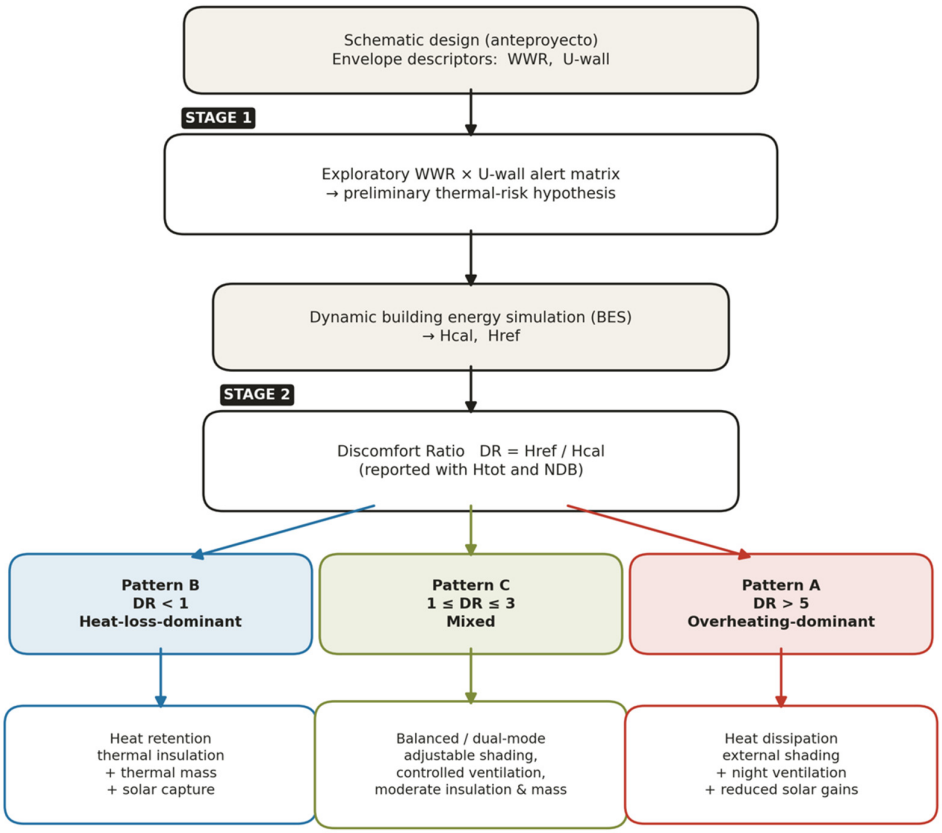


Figure 1. Two-stage exploratory diagnostic framework for early-stage passive design: simple envelope descriptors (WWR and U-wall) are first used to construct a preliminary thermal-risk alert matrix (Stage 1); after dynamic building energy simulation (BES), the Discomfort Ratio (DR = Href/Hcal) confirms the direction of thermal discomfort—heat-loss-dominant, mixed, or overheating-dominant—and supports the selection of passive design strategies—heat-retention (thermal insulation, thermal mass, and useful solar capture) for heat-loss-dominant cases, heat-dissipation (external shading, night ventilation, and reduced solar gains) for overheating-dominant cases, or balanced dual-mode measures (adjustable shading, controlled ventilation, and moderate insulation and thermal mass) for mixed cases (Stage 2). Arrows indicate the sequential diagnostic workflow, from schematic-design envelope descriptors through dynamic simulation to DR-confirmed pattern classification; cell colors distinguish the three DR-confirmed discomfort patterns (blue = heat-loss-dominant, green = mixed, red = overheating-dominant). BES = building energy simulation; DR = Discomfort Ratio; Hcal = unsatisfied heating hours per year; Href = unsatisfied cooling hours per year; U-wall = average thermal transmittance of opaque external walls; WWR = window-to-wall ratio.

2.3. Case Anonymization and Ethical Handling

All cases are reported exclusively through anonymized alphanumeric identifiers (L-01 through L-09 and N-03 through N-17). No student names, surnames, grades, personal identifiers, or other individually identifiable information are disclosed. Only anonymized technical BES outputs are used as analytical data. These outputs were used under institutional academic confidentiality and with authorization from the corresponding academic unit at UTPL. The Discomfort Ratio (DR = Href/Hcal) and the associated discomfort patterns used throughout are defined formally in Section 2.6.

2.4. Variables Analyzed

Seven variables were examined across the 14-case corpus: unsatisfied heating hours per year (Hcal, h/a), unsatisfied cooling hours per year (Href, h/a), the Discomfort Ratio (DR = Href/Hcal), the surface-to-volume ratio (S/V, m^{-1}), the air infiltration rate at 50 Pa (ACH, h^{-1}), the window-to-wall ratio (WWR, %; ratio of total glazed area to total external wall area), and the average thermal transmittance of opaque external walls (U-wall, $W/m^2 \cdot K$). A lower U-wall value indicates lower thermal transmittance—corresponding to higher thermal resistance and a better-insulated opaque assembly—while a higher U-wall value indicates greater heat exchange capacity through the opaque surface. Data completeness varied: DR was available for 13 of 14 cases (N-06 lacked Href data); U-wall for 12; ACH for 8; WWR for 7; and S/V for 6. Missing values were not imputed; all sub-analyses are restricted to cases with valid data for the specific variable, and applicable sample sizes (n) are reported throughout. The air infiltration rate is reported as ACH at 50 Pa (ACH50), a standardized pressurization-test descriptor of envelope airtightness; it is not equivalent to the operational air-change rate under natural pressure differences, nor to an annual ventilation or leakage effect, and in this corpus it largely reflects modeling assumptions rather than measured infiltration. In addition to DR, the total discomfort load (Htot = Href + Hcal) and the Normalized Discomfort Balance (NDB), both defined in Section 2.6, are reported so that the direction and the magnitude of discomfort are assessed jointly.

2.5. Stage 1: Exploratory Envelope-Based Thermal Alert Matrix

For Stage 1 of the diagnostic framework, WWR is categorized as low (<8%), medium (8–20%), or high (>20%), and U-wall as low thermal transmittance (<2.5 $W/m^2 \cdot K$; higher thermal resistance) or high thermal transmittance ($\geq$2.5 $W/m^2 \cdot K$; greater heat-exchange capacity). These category boundaries were not adopted from a single normative source; they were set by the authors as exploratory working bands, informed jointly by the empirical distribution of the corpus and by ranges commonly observed in local Loja construction practice for glazing proportion and for uninsulated versus partially insulated masonry walls. Because such boundaries are not unique, and because the matrix is populated by only six cases, the sensitivity of the cell assignments to small changes in the thresholds is examined explicitly in Section 3.4. The Stage 1 alert matrix is constructed by mapping DR-confirmed outcomes onto the WWR $\times$ U-wall combination cells and is restricted to the six cases for which both variables are available. It is presented as a preliminary hypothesis map derived from a small sample—an exploratory screening device, not a validated predictive model—intended to flag configurations that may warrant attention at the anteproyecto (schematic design) stage, before the architect commits to full dynamic simulation. Its preliminary nature means that discordant cases, in which the matrix alert does not match the DR-confirmed pattern, are expected and diagnostically informative, as they reveal the limits of two-variable screening and the continued necessity of simulation.

2.6. Stage 2: Post-Simulation Discomfort Ratio

The direction of thermal discomfort is characterized by two primary BES outputs: the unsatisfied heating hours per year (Hcal, h/a), defined as the hours in which the simulated indoor operative temperature falls below the lower comfort boundary, and the unsatisfied cooling hours per year (Href, h/a), defined as the hours in which it exceeds the upper comfort boundary. The Discomfort Ratio is defined as

$$DR = H_{ref}/H_{cal} \quad (1)$$

where DR is the Discomfort Ratio, Href the number of unsatisfied cooling hours per year (h/a), and Hcal the number of unsatisfied heating hours per year (h/a). On this basis, three-directional discomfort patterns are defined using corpus-derived exploratory thresholds: Pattern A (overheating-dominant, DR > 5), Pattern B (heat-loss-dominant, DR < 1), and Pattern C (mixed, $1 \leq DR \leq 3$). These boundaries were not adopted from a normative standard or from the prior literature; they were derived from the empirical distribution of DR values within the present corpus, in which a natural directional separation emerged and no case fell within the interval $3 < DR \leq 5$. The thresholds are therefore specific to this dataset and may shift in other corpora; they are intended for exploratory directional classification, not as universal cut-off values, and a threshold-sensitivity check is reported in Section 3.4. Because DR expresses only the direction of thermal imbalance and becomes numerically unstable when Hcal approaches zero—as in the case of L-03, where Hcal = 8 h/a produces DR = 1049—it is reported together with two complementary descriptors. The total discomfort load, Htot = Href + Hcal (h/a), quantifies the overall magnitude of unmet comfort hours independently of direction so that a case with few total discomfort hours is not equated with one carrying a heavy annual load at a similar DR. The Normalized Discomfort Balance, NDB = (Href − Hcal)/(Href + Hcal), is a bounded directional-intensity index ranging from −1 (purely heat-loss-dominant) to +1 (purely overheating-dominant); unlike DR, it remains finite as Hcal approaches zero and allows for the direction and the total load of discomfort to be read jointly. Case N-06 lacked Href data and is therefore not classifiable by DR or NDB; it is retained in Table 1 for documentation but is excluded from all pattern-level analyses.

Table 1. Corpus description: anonymized case identification, thermal discomfort pattern classification, and available morphological and envelope variables. All cases are reported exclusively through alphanumeric identifiers.

ID	Pat.	WWR (%)	S/V (m^{-1})	ACH (h^{-1})	U-Wall ($W/m^2 \cdot K$)	Hcal (h/a)	Href (h/a)	DR
L-01	A	—	—	—	2.61	829	4483	5.41
L-02	B	6	0.646	3.01	5.04	6410	285	0.04
L-03	A	9	0.752	3.93	—	8	8395	1049 †
L-04	A	9	—	—	1.28	173	2325	13.4
L-05	C	18	0.681	3.90	5.41	2243	2645	1.18
L-06	B	7	0.748	4.33	2.46	3449	0	0.00
L-07	C	—	—	—	4.55	2898	4547	1.57
L-08	B	—	—	—	2.76	2647	741	0.28
L-09	A	7	—	—	3.05	87	5269	60.6 ‡
N-03	B	—	—	—	4.14	2213	1476	0.67
N-04	B	—	—	2.47	—	1671	500	0.30
N-06	NC	—	—	4.23	0.33	3789	—	—

Table 1. *Cont.*

ID	Pat.	WWR (%)	S/V (m^{-1})	ACH (h^{-1})	U-Wall ($W/m^2 \cdot K$)	Hcal (h/a)	Href (h/a)	DR
N-12	C	—	0.574	2.74	4.71	851	2067	2.43
N-17	A	33	0.143	1.22	1.68	292	6988	23.9

Note: — = data not available; Hcal = unsatisfied heating hours per year (h/a); Href = unsatisfied cooling hours per year (h/a); DR = Href/Hcal; WWR = window-to-wall ratio (%); ACH = air changes per hour at 50 Pa (h^{-1}); S/V = surface-to-volume ratio (m^{-1}); U-wall = average thermal transmittance of opaque external walls ($W/m^2 \cdot K$); lower U-wall values indicate lower thermal transmittance and a better-insulated opaque envelope; Pat. = thermal discomfort pattern; Pattern A = overheating-dominant; Pattern B = heat-loss-dominant; Pattern C = mixed; NC = not classifiable due to missing DR data. † Extreme value (Hcal = 8 h/a); interpret with caution. ‡ Extreme DR at low WWR; discussed in Section 3.5.

2.7. Analytical Approach

The corpus size (total n = 14; classifiable n = 13) is appropriate for exploratory configurational study, in which the aim is not statistical generalization, but the identification of recurrent variable-state combinations and directional tendencies [23]; inferential methods would be underpowered for this corpus, and are therefore not applied [24]. A configurational analysis [23,25] is therefore adopted, focusing on the variable-state combinations consistently associated with each outcome pattern. For each variable, the median and range are reported per pattern group. Missing values are not imputed, and each sub-analysis is restricted to the cases with valid data for the variable in question. No significance tests are reported, and no causal claims are made.

3. Results

3.1. Corpus Description and DR Pattern Distribution

Table 1 presents the 14-case corpus. Of the 13 classifiable cases, 5 were assigned to Pattern A, 5 to Pattern B, and 3 to Pattern C. Case N-06 lacked Href data and could not be assigned a DR value; it is retained in Table 1 for documentation but is excluded from all pattern-level analyses. Case L-03 shows an extreme DR (1049) that reflects a near-zero Hcal (8 h/a); it too is retained for documentation but is interpreted with caution. Case L-09 shows DR = 60.6 at a low WWR (7%) and a moderate U-wall (3.05 $W/m^2 \cdot K$) and does not fit neatly into either the solar-gain or heat-retention pathway discussed in Section 3.5. It illustrates that a low WWR alone does not guarantee protection against overheating when other factors—building orientation, roof exposure, thermal mass, internal loads, or ventilation assumptions—are not controlled simultaneously. Figure 2 provides a schematic representation of the three discomfort patterns defined by the DR.

Reading direction and magnitude jointly confirm and refine the DR classification. The total discomfort load (Htot = Href + Hcal) ranges from about 2200 to 8400 h/a across the corpus and is not aligned with DR: case L-03, whose DR of 1049 is an artifact of a near-zero Hcal (8 h/a), carries one of the highest total loads (8403 h/a), whereas case L-04 reaches a high DR (13.4) at a comparatively modest load (2498 h/a). The Normalized Discomfort Balance (NDB) places every classifiable case on a bounded −1 to +1 scale and removes the instability of DR at low Hcal: the five Pattern A cases all fall in the strongly positive range (NDB ≈ +0.69 to +1.00, including L-03 at +1.00 and L-09 at +0.97, which, on the DR scale, appeared as extreme outliers at 1049 and 60.6); the five Pattern B cases are all negative (NDB ≈ −0.20 to −1.00); and the three Pattern C cases cluster near zero (NDB ≈ +0.08 to +0.42). Direction is thus preserved, while the apparent extremity of L-03 and L-09 is shown to be a scaling effect of the ratio rather than a difference in kind.

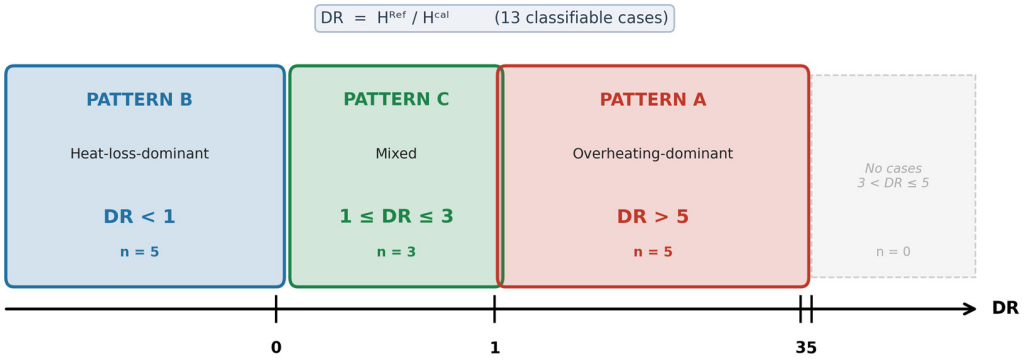


Figure 2. Stage 2 directional classification: three thermal discomfort patterns defined by the Discomfort Ratio (DR = Href/Hcal). Pattern A (overheating-dominant, DR > 5), Pattern B (heat-loss-dominant, DR < 1), and Pattern C (mixed, $1 \leq DR \leq 3$). The interval $3 < DR \leq 5$ contained no cases in this corpus. Case counts: Pattern A n = 5, Pattern B n = 5, Pattern C n = 3 (total classifiable n = 13; NC n = 1). DR = Discomfort Ratio; Hcal = unsatisfied heating hours per year; Href = unsatisfied cooling hours per year; NC = not classifiable.

3.2. S/V and ACH Do Not Discriminate Between Patterns

Table 2 summarizes the median and range of each variable by pattern. The S/V ratio has medians of 0.448 (Pattern A, n = 2), 0.697 (Pattern B, n = 2), and 0.628 (Pattern C, n = 2), with substantially overlapping ranges. ACH has medians of 2.58, 3.01, and 3.32 h^{-1} for Patterns A, B, and C, respectively—again overlapping. Within the available sub-samples, neither S/V nor ACH shows a systematic directional relationship with the assigned discomfort pattern in this corpus.

Table 2. Median and range of morphological and envelope variables by thermal discomfort pattern. Values: median (range: min–max) for cases with valid data; n denotes the sub-sample with valid data for each variable–pattern combination.

Variable	Pattern A—Overheating-Dominant (n = 5)	Pattern B—Heat-Loss-Dominant (n = 5)	Pattern C—Mixed (n = 3)
S/V ratio (m^{-1})	0.448 (range: 0.143–0.752; n = 2)	0.697 (range: 0.646–0.748; n = 2)	0.628 (range: 0.574–0.681; n = 2)
ACH @50 Pa (h^{-1})	2.575 (range: 1.22–3.93; n = 2)	3.01 (range: 2.47–4.33; n = 3)	3.32 (range: 2.74–3.90; n = 2)
WWR (%)	9.0 (range: 7–33; n = 4)	6.5 (range: 6–7; n = 2)	18.0 (n = 1, single case)
U-wall ($W/m^2 \cdot K$)	2.15 (range: 1.28–3.05; n = 4)	3.45 (range: 2.46–5.04; n = 4)	4.71 (range: 4.55–5.41; n = 3)

Note: Lower U-wall values indicate lower thermal transmittance (better-insulated opaque envelope); higher values indicate greater heat exchange capacity through the opaque surface. Sub-sample sizes reflect data availability and do not sum to the total classifiable corpus (n = 13) for any single variable. ACH = air changes per hour; S/V = surface-to-volume ratio; U-wall = average thermal transmittance of opaque external walls; WWR = window-to-wall ratio.

3.3. Stage 1: WWR and U-Wall as Preliminary Alert Descriptors

WWR and U-wall serve as the Stage 1 descriptors because they are available at the anteproyecto stage and, in this corpus, show clearer directional associations with the DR-confirmed pattern than S/V or ACH (Table 2). Both Pattern B cases with WWR data (L-02, 6%; L-06, 7%) have consistently low values, and the only Pattern C case with WWR data is L-05 (18%). Pattern A cases span a wide range (7–33%; median 9.0%), indicating that overheating-dominant behavior is not confined to high glazing ratios—a result with direct design implications, since it rules out prescriptive glazing limits as a sufficient stand-alone strategy. Figure 3 plots the unsatisfied cooling hours (Href) against the unsatisfied heating hours (Hcal) for the 13 classifiable cases, with dashed diagonal lines marking the constant DR thresholds that separate the three discomfort patterns.

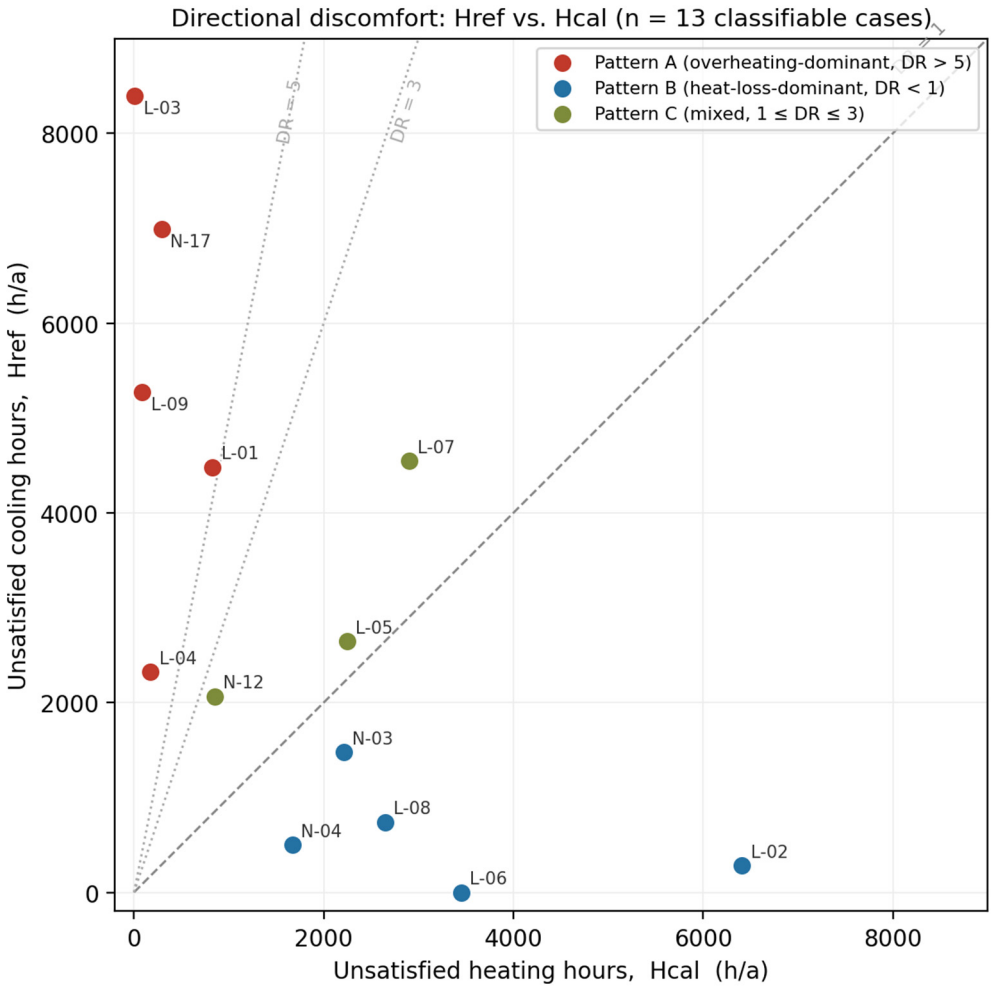


Figure 3. Directional discomfort plot showing unsatisfied cooling hours (Href, y-axis) versus unsatisfied heating hours (Hcal, x-axis) for the 13 classifiable cases. Dashed diagonal lines indicate constant Discomfort Ratio (DR = Href/Hcal) thresholds—DR = 1, DR = 3, and DR = 5—used to distinguish Pattern B (heat-loss-dominant), Pattern C (mixed), and Pattern A (overheating-dominant). Marker color denotes the DR-confirmed discomfort pattern. DR = Discomfort Ratio; Hcal = unsatisfied heating hours per year; Href = unsatisfied cooling hours per year.

3.4. Stage 1 Matrix and Stage 2 DR Confirmation

U-wall shows an inverse distributional pattern relative to overheating tendency: Pattern A cases have the lowest median U-wall (2.15 W/m^2·K; lower thermal transmittance), Pattern B cases higher values (3.45 W/m^2·K), and Pattern C cases have the highest (4.71 W/m^2·K; Table 2). This inverse relationship—in which lower-thermal-transmittance, better-insulated opaque envelopes are associated with overheating rather than heat-loss dominance—is counterintuitive from a conventional energy efficiency standpoint and warrants careful interpretation. A plausible explanation is a heat-retention mechanism arising from the combined action of high thermal insulation (a low thermal transmittance that slows conductive heat exchange through the assembly) and thermal mass (the capacity of the construction to store heat during the day and re-release it later): where the principal thermal driver is solar radiation rather than extreme outdoor air temperature, a low thermal transmittance opaque surface may limit not only daytime heat gain through the assembly, but also the building's capacity to release heat overnight so that solar gains through the glazing and internal loads can accumulate through the night. This behavior is consistent with effects reported for low-thermal-mass well-insulated buildings in mixed-climate contexts [23,26]. It remains a descriptive hypothesis consistent with the observed distribution;

the variables available in this corpus do not allow for the mechanism to be isolated or demonstrated causally. Table 3 presents the Stage 1 alert matrix, which combines the WWR and U-wall categories and maps the Stage 2 DR-confirmed outcomes onto each cell.

Table 3. Exploratory configurational matrix: combinations of WWR category and U-wall category versus observed thermal discomfort pattern, based on the six cases with both variables available (n = 6). Low thermal transmittance: U-wall < 2.5 W/m^2·K (higher thermal resistance); high thermal transmittance: U-wall ≥ 2.5 W/m^2·K (greater heat exchange capacity through opaque surface). The glazing descriptors low, moderate, and high denote window-to-wall ratio (WWR, glazed-area proportion) bands—low (<8%), moderate (8–20%), and high (>20%)—and not the thermal properties of the glazing itself; the glazing thermal transmittance (Ug) and whole-window U-value (Uw) were not uniformly documented in the corpus and are to be specified where available (see Section 4.4).

Configuration (WWR × U-Wall)	Observed Pattern	Representative Cases	Exploratory Physical Interpretation
WWR < 8%/U-wall < 2.5 W/m^2·K (low thermal transmittance)	Pattern B	L-06 (WWR = 7%, U = 2.46 W/m^2·K)	Low glazing + low thermal transmittance opaque envelope. Heat-loss tendency observed. Single-case cell; interpret with caution.
WWR < 8%/U-wall ≥ 2.5 W/m^2·K (high thermal transmittance)	B and A (ambiguous)	L-02 (B, WWR = 6%, U = 5.04); L-09 (A, WWR = 7%, U = 3.05)	Low glazing + high thermal transmittance opaque envelope. Ambiguous outcome. Orientation, thermal mass, or ventilation assumptions likely determinant.
WWR 8–20%/U-wall < 2.5 W/m^2·K (low thermal transmittance)	Pattern A	L-04 (WWR = 9%, U = 1.28 W/m^2·K)	Moderate glazing + low thermal transmittance opaque envelope. Overheating tendency. Possible heat retention from the combination of high thermal insulation and thermal mass, which limits nighttime heat release. Single-case cell.
WWR 8–20%/U-wall ≥ 2.5 W/m^2·K (high thermal transmittance)	Pattern C	L-05 (WWR = 18%, U = 5.41 W/m^2·K)	Moderate glazing + high thermal transmittance opaque envelope. Mixed discomfort pattern. Single-case cell.
WWR > 20%/U-wall < 2.5 W/m^2·K (low thermal transmittance)	Pattern A	N-17 (WWR = 33%, U = 1.68 W/m^2·K)	High glazing + low thermal transmittance opaque envelope. Strong overheating tendency. High solar gains combined with limited heat dissipation, as the high thermal insulation and thermal mass of the opaque envelope restrict nighttime heat release.
WWR > 20%/U-wall ≥ 2.5 W/m^2·K (high thermal transmittance)	No data	—	No case in the corpus presents this configuration. Outcome unknown.

Note: All cells contain only one or two cases; no cell is statistically representative. Interpretations are exploratory physical hypotheses, not established causal mechanisms. The ambiguous cell (low WWR/high thermal transmittance) demonstrates that these two variables do not fully determine the discomfort pattern. U-wall = average thermal transmittance of opaque external walls; WWR = window-to-wall ratio.

Table 3 presents the exploratory configurational matrix for the six cases with both WWR and U-wall data, and Figure 4 provides a schematic representation. Five of the six possible cells are populated. The most notable feature is the ambiguous cell (low WWR/high thermal transmittance U-wall), in which L-02 follows Pattern B and L-09 follows Pattern A, showing that WWR and U-wall together do not uniquely determine the discomfort pattern in every configuration and that additional factors are operative.

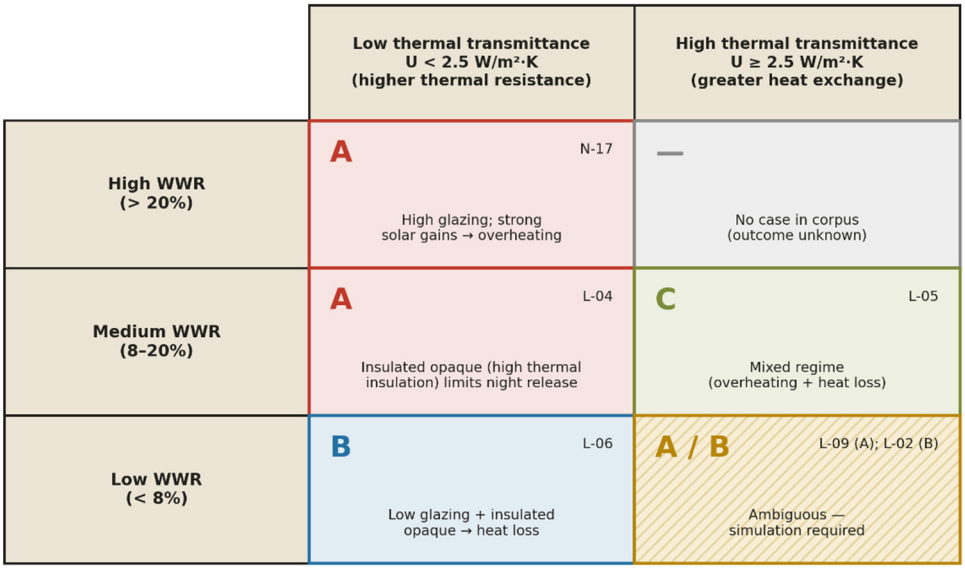


Figure 4. Stage 1 alert matrix: WWR × U-wall exploratory configurational matrix. Each cell shows the Stage 2 DR-confirmed thermal discomfort pattern(s) and corresponding case(s) from the corpus (n = 6 cases with both variables). The ambiguous cell (low WWR/high thermal transmittance) contains both Pattern A (L-09) and Pattern B (L-02) outcomes, demonstrating that the Stage 1 matrix does not replace dynamic simulation. DR = Discomfort Ratio; U-wall = average thermal transmittance of opaque external walls; WWR = window-to-wall ratio.

The robustness of these cell assignments to the chosen category boundaries was checked directly. Two cases lie close to a threshold: L-06 has U-wall = 2.46 W/m^2·K, essentially on the 2.5 W/m^2·K cut-off, and L-04 has WWR = 9%, just above the 8% low/medium boundary. Raising the U-wall cut-off slightly would move L-06 into the high-thermal-transmittance column and empty the low-WWR/low-thermal-transmittance cell; raising the WWR boundary to 10% would move L-04 into the low-WWR band, where it would join L-06 and create a second ambiguous (A versus B) cell. The remaining assignments (L-02, L-05, L-09, N-17) are stable under comparable shifts. With only six cases, individual cell contents are therefore sensitive to the exact boundaries and should be read as provisional, which reinforces the interpretation of the matrix as a preliminary hypothesis map rather than a fixed classification.

3.5. Discordant Cases and Limits of the Alert Matrix

Table 4 presents the five Pattern A cases individually. The group is heterogeneous: among cases with data, WWR ranges from 7% to 33% and U-wall from 1.28 to 3.05 W/m^2·K (lower values indicate lower thermal transmittance). Two tentative overheating pathways can be suggested, although neither can be confirmed without additional variables.

Table 4. Pattern A cases: Available envelope and simulation data with interpretive notes on possible overheating mechanisms. Interpretations are tentative; they require additional variables for confirmation.

Case	WWR (%)	U-Wall (W/m^2·K)	Hcal (h/a)	Href (h/a)	DR/Interpretive Note
L-01	—	2.61	829	4483	5.41—No WWR data. Mechanism undetermined.
L-03	9	—	8	8395	1049—Extreme outlier (Hcal = 8 h/a). Excluded from mechanism discussion.
L-04	9	1.28	173	2325	13.4—Low-thermal-transmittance opaque envelope (U = 1.28 W/m^2·K); moderate WWR. Consistent with heat-retention hypothesis.
L-09	7	3.05	87	5269	60.6—Extreme DR at low WWR and moderate U-wall. Other factors likely operative.
N-17	33	1.68	292	6988	23.9—High WWR (33%) + low thermal transmittance envelope. Solar-gain mechanism dominant.

Note: — = data not available; DR = Discomfort Ratio; Hcal = unsatisfied heating hours per year (h/a); Href = unsatisfied cooling hours per year (h/a); U-wall = average thermal transmittance of opaque external walls (W/m^2·K); WWR = window-to-wall ratio (%).

Solar-gain pathway: Case N-17 (WWR = 33%, U-wall = 1.68 W/m^2·K) has an extreme glazing ratio for this climate. High solar gains through the large, glazed area are the most plausible explanation for its overheating-dominant profile (DR = 23.9), possibly amplified by the relatively low thermal transmittance opaque envelope, which limits heat release.

Heat-retention pathway (hypothetical): Case L-04 (WWR = 9%, U-wall = 1.28 W/m^2·K) combines low glazing with a very low thermal transmittance opaque envelope. Its overheating-dominant DR (13.4) is unlikely to be driven mainly by solar gains through glazing. One interpretation is that the well-insulated opaque envelope limits nighttime heat dissipation, allowing for daytime solar and internal loads to accumulate without adequate passive release. This hypothesis cannot be confirmed from the available data.

Because two Pattern A cases carry extreme DR values, their influence on the group-level interpretation was tested by leave-one-out analysis. Removing L-03 (DR = 1049) leaves Pattern A with four cases and changes the group median DR only marginally (from 23.9 to about 18.7); because L-03 contributes no U-wall value, the inverse U-wall finding for Pattern A (median 2.15 W/m^2·K) is unaffected and the overheating-dominant interpretation is unchanged. Removing L-09 has a more specific effect: the ambiguous low-WWR/high-thermal-transmittance cell of the Stage 1 matrix then contains only L-02 (Pattern B) and is no longer ambiguous. The qualitative claim that two descriptors do not uniquely determine the discomfort pattern therefore rests substantially on L-09. This is fully consistent with the study's central argument—that low WWR alone does not guarantee protection against overheating and that dynamic simulation remains necessary—but the single-case basis of the ambiguous cell is acknowledged as a limitation.

3.6. Practical Architectural Implications

Table 5 synthesizes the configurational observations into exploratory passive-design implications for residential buildings in NEC Climate Zone 3. These implications derive from corpus associations, and are not intended as normative prescriptions or validated design thresholds; the WWR and U-wall ranges given are descriptive reference ranges from the corpus, not recommended target values.

Table 5. Practical use of the two-stage diagnostic framework for early-stage architectural decision-making. Stage 1 (preliminary alert) is based on WWR and U-wall; Stage 2 (DR-confirmed pattern) is derived from post-simulation Discomfort Ratio. Interpretations are exploratory and corpus-specific; no cell constitutes a normative design prescription.

Stage 1 Preliminary Alert	Typical Envelope Configuration Observed in Corpus	Stage 2 DR-Confirmed Pattern	Architectural Interpretation	Possible Passive Design Response	Caution
Possible heat-loss alert	Low WWR (<8%); U-wall variable or high thermal transmittance cases	Pattern B, DR < 1	Limited solar aperture and/or high heat exchange may favor cold-side discomfort.	Review useful solar gains; reduce uncontrolled infiltration; improve envelope continuity; evaluate moderate insulation and thermal mass.	Based on small sub-samples (n = 2 for WWR); WWR and U-wall alone do not determine the outcome.
Possible mixed dual-pressure condition	Medium WWR (8–20%) with high thermal transmittance opaque envelope	Pattern C, $1 \leq DR \leq 3$	Both overheating and heat-loss discomfort coexist.	Use balanced strategies: controllable solar protection, moderate glazing, thermal mass, controlled ventilation.	Only one Pattern C case has WWR data; requires validation in larger corpus.
Possible overheating alert	High WWR (>20%) and/or low thermal transmittance opaque envelope (U-wall < 2.5 $W/m^2 \cdot K$)	Pattern A, DR > 5	Solar gains or heat-retention effects may dominate.	Reduce excessive solar gains; add shading; improve night ventilation; assess thermal mass and window SHGC.	Pattern A is heterogeneous; L-09 shows that overheating can occur even at low WWR, so dynamic simulation is always required.
Discordant/ uncertain alert	Low WWR + moderate U-wall, or incomplete variable set	Variable (see discordant case L-09)	Other factors may dominate, including orientation, roof exposure, internal gains, thermal mass, ventilation.	Do not decide from matrix alone; proceed to dynamic BES and sensitivity analysis.	The matrix is a screening tool, not a predictive model. L-09 (DR = 60.6 at WWR = 7%) demonstrates the limits of two-variable screening.

Note: All observed ranges are based on small sub-samples (see values in Table 2). The caution statements in the rightmost column are integral to the interpretation of each row. BES = building energy simulation; DR = Discomfort Ratio; SHGC = solar heat gain coefficient; U-wall = average thermal transmittance of opaque external walls; WWR = window-to-wall ratio.

4. Discussion

4.1. From Envelope Description to Thermal-Risk Alert

The Stage 1 alert matrix operationalizes a simple architectural insight: before committing to dynamic simulation, an architect can infer the likely direction of thermal risk from two envelope descriptors—WWR and U-wall—available at the anteproyecto stage. This is not prediction; it is a structured way to organize preliminary design intuitions and to flag configurations likely to require heat-retention, heat-dissipation, or balanced passive strategies before simulation confirms the direction. The non-discriminatory behavior of S/V and ACH in this corpus is itself relevant to the matrix design: because these variables yield no useful preliminary alert, they are not included in Stage 1.

The absence of discriminating configurational associations for S/V and ACH is consistent with the argument that geometric compactness predicts performance more reliably in climates with a single dominant thermal driver than in climates under dual thermal pressure [8,9,27,28]. In heating-dominated contexts, compact form reduces total envelope area and limits conductive heat loss in a largely unidirectional way. In high-altitude temperate Andean climates such as Loja, however, overheating and heat-loss risks coexist, and therefore reducing envelope area through compactness limits heat loss and heat dissipation without distinguishing between them. The net effect on DR is therefore not predictable from S/V alone, which explains the overlapping distributions across Patterns A, B, and C in this corpus. This does not imply that geometric form is irrelevant to thermal performance, but rather that S/V alone is insufficient to discriminate the direction of discomfort in this climatic context.

The non-discriminating behavior of ACH may reflect two factors. First, the narrow effective range observed in the corpus (approximately 1.2–5.0 h^{-1} at 50 Pa) may be too small to produce strongly differentiated DR outcomes under the mild temperature differentials in this climate. Second, infiltration increases heat loss in cold periods while providing incidental passive cooling in warm periods, so its net effect on DR may be approximately neutral across the observed range [29]. In addition, the ACH values in this corpus likely reflect modeling assumptions rather than measured infiltration, further reducing their discriminating potential.

4.2. The Alert Matrix as a Screening Tool, Not a Predictive Model

The directional association between WWR and the discomfort pattern is consistent with established findings on the glazing-ratio effects in residential buildings under mixed climates [14,15,26]: a lower WWR limits solar heat gain and favors heat-loss-dominant behavior, whereas a higher WWR increases net solar gains and is associated with mixed or overheating-dominant outcomes. The wide WWR range among Pattern A cases (7–33% among cases with data), spanning low to very high glazing ratios, indicates that overheating is not produced exclusively by excessive solar aperture. This reinforces the need to consider WWR and U-wall jointly, rather than as independent prescriptive parameters, in early-stage passive design for this climate.

4.3. The DR as a Post-Simulation Directional Index

The Discomfort Ratio (DR = Href/Hcal) translates dynamic BES outputs into a directional design decision: Pattern B configurations (DR < 1) indicate that heat-retention strategies are the priority, whereas Pattern A configurations (DR > 5) call for heat-dissipation measures; Pattern C ($1 \leq DR \leq 3$) calls for balanced, dual-mode strategies that address overheating and heat loss together. This directional reading distinguishes the DR from aggregate indicators such as annual energy use intensity, which do not reveal the direction of discomfort and therefore cannot guide the choice of specific passive responses.

The inverse distributional relationship between U-wall and overheating tendency in this corpus—Pattern A cases having the lowest median U-wall (2.15 $W/m^2 \cdot K$)—illustrates how the DR can reveal counterintuitive configurations that aggregate indicators would not flag. A plausible physical explanation is a heat-retention mechanism: in solar-driven climates, well-insulated opaque envelopes may limit not only daytime heat gain through the opaque surface, but also the building's capacity to dissipate heat overnight, allowing for thermal accumulation when solar gains or internal loads are present. This remains a descriptive hypothesis consistent with the observed distribution; the available variables do not allow for the mechanism to be confirmed causally. Stronger interpretive

claims would require additional data on thermal mass, ventilation rates, occupancy, and building orientation.

From a normative standpoint, the NEC-HS-EE prescribes maximum U-wall values for Climate Zone 3. The present findings do not challenge those requirements; rather, they suggest that U-wall should be interpreted together with ventilation, thermal mass, and solar control when assessing the direction of discomfort in dual-pressure climates. Larger, controlled datasets are needed before any regulatory implications can be drawn.

4.4. Limitations and Future Validation

Several limitations constrain the scope of this study and of the diagnostic framework it proposes. First, the corpus (total n = 14; classifiable n = 13) is adequate for exploratory configurational analysis, but insufficient for statistical inference; all reported associations are descriptive and corpus-specific, and the corpus derives from course-based academic BES projects rather than a purpose-designed experimental protocol. Second, data completeness is uneven: S/V and WWR are available for only six and seven cases, respectively, reducing the effective sub-samples to as few as a 1–2 per variable-pattern combination, and the Stage 1 matrix is restricted to six cases. Third, several key determinants of thermal discomfort—building orientation, roof exposure, thermal mass, window solar heat gain coefficient (SHGC), external shading, and actual ventilation schedules—were not uniformly documented and are absent from the Stage 1 matrix, which limits interpretive confidence, particularly for discordant cases such as L-09. Fourth, the corpus was not compiled under a unified simulation protocol, so heterogeneity in modeling assumptions may introduce errors that cannot be quantified. Fifth, the BES outputs were not validated against measured indoor temperature or energy data. Sixth, the geographic scope is limited to Loja, and the findings should not be transferred to other high-altitude Andean cities without empirical validation. Seventh, the glazing in the corpus is described only through the window-to-wall ratio (a glazed-area proportion); the thermal properties of the glazing itself—glazing thermal transmittance (Ug) and whole-window U-value (Uw), together with the solar heat gain coefficient—were not uniformly documented, so the WWR bands used in Stage 1 capture the size of the glazed aperture but not its thermal quality. Documenting Ug, Uw, and SHGC in future corpora would allow the Stage 1 descriptors to distinguish glazing area from glazing thermal performance and would refine the alert matrix accordingly.

Validating the two-stage framework will require extending the corpus to 30 or more cases with complete, validated envelope data; applying a unified BES protocol; incorporating orientation, roof exposure, thermal mass, and SHGC as configurational variables in a refined Stage 1 matrix; and benchmarking Stage 2 DR values against measured indoor data.

5. Conclusions

This study proposed a two-stage exploratory diagnostic framework for early-stage passive design in high-altitude Andean residential buildings (14 BES cases in Loja, Ecuador, NEC Climate Zone 3; 13 classifiable by DR; 6 with complete WWR and U-wall data for the Stage 1 matrix). Stage 1 uses WWR and U-wall as simple envelope descriptors to build a preliminary thermal-risk alert matrix; Stage 2 uses the Discomfort Ratio (DR = Href/Hcal), computed after dynamic BES, to confirm the direction of thermal discomfort as overheating-dominant, heat-loss-dominant, or mixed. The conclusions below reflect the exploratory, corpus-specific nature of the findings; validation in larger, purpose-designed datasets is required before any normative or predictive use. In application, the two stages operate as a single sequential decision workflow: at the anteproyecto stage the architect reads the WWR × U-wall alert matrix to anticipate the likely direction of thermal risk; after dynamic BES, the DR (read together with NDB and Htot) confirms that direction; and only

then is the corresponding passive strategy selected—heat retention for heat-loss-dominant cases, heat dissipation for overheating-dominant cases, or balanced dual-mode measures for mixed cases. This explicit coupling of method and application is what distinguishes the framework from aggregate energy indicators, which do not resolve the direction of discomfort and therefore cannot guide the choice of passive response.

Within this corpus, the geometric morphological variables—surface-to-volume ratio and air infiltration rate—show substantially overlapping distributions across thermal discomfort patterns and no discriminative configurational association with the direction of discomfort. This suggests that morphological compactness alone is insufficient as a passive-design criterion for thermal comfort in high-altitude temperate Andean residential buildings, where overheating and heat-loss risk operate across the same annual cycle.

The window-to-wall ratio shows a directional, descriptive association with the discomfort pattern: heat-loss-dominant cases have low WWR (6–7% in the two cases with data), the single Pattern C case with WWR data has a moderate value (18%), and overheating-dominant cases span a wide range (7–33%), indicating that overheating arises through more than one configurational pathway.

Opaque-wall thermal transmittance shows an inverse distributional pattern: overheating-dominant cases have the lowest median U-wall (2.15 $W/m^2 \cdot K$—lower thermal transmittance, better-insulated assemblies) compared with heat-loss-dominant (3.45 $W/m^2 \cdot K$) and mixed (4.71 $W/m^2 \cdot K$) cases. This is consistent with a possible heat-retention mechanism in which well-insulated opaque assemblies limit nighttime heat dissipation; however, the available variables do not allow for the mechanism to be isolated or demonstrated causally, and it remains a descriptive hypothesis requiring validation.

For Stage 1 of the framework, the exploratory WWR $\times$ U-wall alert matrix (n = six cases with both variables) identifies directionally consistent pattern associations in four populated cells, with one ambiguous cell (L-09 versus L-02 at low WWR) showing that these two descriptors do not uniquely determine the discomfort pattern in all configurations. The matrix is a preliminary screening tool to guide early-stage passive design decisions, not a validated predictive model; dynamic simulations remain necessary.

In summary, the study contributes a practice-oriented, two-stage exploratory workflow for schematic (anteproyecto) design in high-altitude Andean residential buildings. The method couples a Stage 1 alert matrix built from two descriptors available before simulation (WWR and U-wall) with a Stage 2 post-simulation reading of discomfort direction (DR), reported together with a bounded directional-intensity index (NDB) and the total discomfort load (Htot). Its intended application is deliberately narrow: to help an architect anticipate, and then confirm, whether a given configuration tends toward overheating, heat loss, or a mixed regime, and thereby prioritize heat-dissipation, heat-retention, or balanced passive strategies, not to predict absolute performance or to set normative limits. Within this corpus, S/V and ACH did not discriminate across patterns, the matrix produced useful but non-unique alerts, and the discordant case L-09 (overheating-dominant at low WWR) marks the limit of two-variable screening and the continued necessity of dynamic simulation. Realizing the method as a transferable design aid will require validation on larger, purpose-built datasets (30 or more cases) under a unified BES protocol, incorporating orientation, roof exposure, thermal mass, SHGC, and real ventilation rates, as well as benchmarking simulation outputs against measured indoor data.

Author Contributions: Conceptualization, R.C.-J. and M.T.-G.; methodology, R.C.-J. and M.T.-G.; data curation, R.C.-J.; formal analysis, R.C.-J.; investigation, R.C.-J. and M.T.-G.; writing—original draft preparation, R.C.-J.; writing—review and editing, M.T.-G. and R.C.-J.; supervision, M.T.-G.; project administration, R.C.-J. All authors have read and agreed to the published version of the manuscript.

Funding: This research received no external funding.

Institutional Review Board Statement: Not applicable. This study did not involve human participants, surveys, interviews, interventions, personal data, identifiable student data, occupant information, or human-subject research. The analytical corpus consists exclusively of anonymized technical building energy simulation outputs generated as part of regular academic coursework in the Environmental Analysis of Buildings course, Architecture program, Universidad Técnica Particular de Loja (UTPL), during the October 2025–February 2026 academic period. All cases are reported using anonymized alphanumeric identifiers. No student names, academic grades, personal identifiers, occupant information, or individually identifiable information are disclosed in the manuscript, tables, figures, or captions. The use of anonymized outputs was conducted under institutional academic confidentiality and with authorization from the corresponding academic unit at UTPL.

Informed Consent Statement: Not applicable. The study did not involve human participants, personal data, surveys, interviews, or identifiable information.

Data Availability Statement: The aggregated building energy simulation outputs and corpus variables analyzed in this study are available from the corresponding author upon reasonable request. Individual project documentation from the Environmental Analysis of Buildings course is retained under institutional academic confidentiality and is not publicly distributed. No personal data of students, occupants, or other individuals are included in the dataset. Data were not deposited in a public repository due to institutional confidentiality constraints on course-based academic materials.

Acknowledgments: The authors acknowledge the academic context of the Environmental Analysis of Buildings course at Universidad Técnica Particular de Loja (UTPL) during the October 2025–February 2026 academic period, from which the anonymized simulation-based case corpus was derived.

Conflicts of Interest: The authors declare no conflicts of interest.

Abbreviations

Abbreviation	Definition
ACH	Air changes per hour
BES	Building energy simulation
DR	Discomfort Ratio
EPW	EnergyPlus Weather file
Hcal	Unsatisfied heating hours per year
HDD	Heating degree days
Href	Unsatisfied cooling hours per year
NEC	Norma Ecuatoriana de la Construcción
NEC-HS-EE	NEC—Habitabilidad y Salud: Eficiencia Energética
S/V	Surface-to-volume ratio
SHGC	Solar heat gain coefficient
U-wall	Average thermal transmittance of opaque external walls ($W/m^2 \cdot K$)
UTPL	Universidad Técnica Particular de Loja
WWR	Window-to-wall ratio

References

1. World Health Organization. *WHO Housing and Health Guidelines*; WHO Press: Geneva, Switzerland, 2018. Available online: https://www.who.int/publications/i/item/9789241550376 (accessed on 29 April 2026).
2. Fanger, P.O. *Thermal Comfort: Analysis and Applications in Environmental Engineering*; Danish Technical Press: Copenhagen, Denmark, 1970.
3. IEA. *World Energy Outlook 2023*; International Energy Agency: Paris, France, 2023. Available online: https://www.iea.org/reports/world-energy-outlook-2023 (accessed on 29 April 2026).
4. Hensen, J.L.M.; Lamberts, R. (Eds.) *Building Performance Simulation for Design and Operation*, 2nd ed.; Routledge: London, UK, 2019. [CrossRef]
5. ASHRAE. *ASHRAE Standard 55-2023: Thermal Environmental Conditions for Human Occupancy*; ASHRAE: Atlanta, GA, USA, 2023.

6. Crawley, D.B.; Lawrie, L.K.; Winkelmann, F.C.; Buhl, W.F.; Huang, Y.J.; Pedersen, C.O.; Strand, R.K.; Liesen, R.J.; Fisher, D.E.; Witte, M.J.; et al. EnergyPlus: Creating a new-generation building energy simulation program. *Energy Build.* **2001**, *33*, 319–331. [CrossRef]
7. Torcellini, P.; Pless, S.; Deru, M.; Crawley, D. *Zero Energy Buildings: A Critical Look at the Definition*; NREL/CP-550-39833; National Renewable Energy Laboratory: Golden, CO, USA, 2006. Available online: https://www.nrel.gov/docs/fy06osti/39833.pdf (accessed on 29 April 2026).
8. Depecker, P.; Menezo, C.; Virgone, J.; Lepers, S. Design of buildings shape and energetic consumption. *Build. Environ.* **2001**, *36*, 627–635. [CrossRef]
9. Danielski, I.; Fröling, M.; Joelsson, A. The impact of the shape factor on final energy demand in residential buildings in Nordic climates. In Proceedings of the World Renewable Energy Forum (WREF 2012), Denver, CO, USA, 13–17 May 2012; pp. 4260–4264. Available online: https://www.diva-portal.org/smash/get/diva2:532979/fulltext01.pdf (accessed on 29 April 2026).
10. Bustamante, W.; Uribe, D.; Vera, S.; Molina, G. An integrated thermal and lighting simulation tool to support the design process of complex fenestration systems for office buildings. *Appl. Energy* **2017**, *198*, 36–48. [CrossRef]
11. Barbosa, R.; Vicente, R.; Santos, R. Climate change and thermal comfort in Southern European housing: A case study from Lisbon. *Build. Environ.* **2015**, *92*, 440–451. [CrossRef]
12. Auliciems, A.; Szokolay, S.V. *Thermal Comfort*, 2nd ed.; PLEA International: Brisbane, Australia, 2007.
13. Ministerio de Desarrollo Urbano y Vivienda (MIDUVI). *Norma Ecuatoriana de la Construcción—NEC-HS-EE: Eficiencia Energética en la Construcción en Ecuador*; MIDUVI: Quito, Ecuador, 2019.
14. Goia, F. Search for the optimal window-to-wall ratio in office buildings in different European climates and the implications on total energy saving potential. *Sol. Energy* **2016**, *132*, 467–492. [CrossRef]
15. Acosta, I.; Campano, M.A.; Molina, J.F. Window design in architecture: Analysis of energy savings for lighting and visual comfort in residential spaces. *Appl. Energy* **2016**, *168*, 493–506. [CrossRef]
16. Kaynakli, O. A study on residential heating energy requirement and optimum insulation thickness. *Renew. Energy* **2008**, *33*, 1164–1172. [CrossRef]
17. Al-Sanea, S.A.; Zedan, M.F. Improving thermal performance of building walls by optimizing insulation layer distribution and thickness for same thermal mass. *Appl. Energy* **2011**, *88*, 3113–3123. [CrossRef]
18. Nicol, F.; Humphreys, M.; Roaf, S. *Adaptive Thermal Comfort: Principles and Practice*; Earthscan: London, UK, 2012.
19. Cheng, R.; Zhang, N.; Zhang, W.; Sun, Y.; Yin, B.; Gao, W. Impact of Thermal Mass, Window Performance, and Window–Wall Ratio on Indoor Thermal Dynamics in Public Buildings. *Buildings* **2025**, *15*, 1757. [CrossRef]
20. Delgado-Gutiérrez, E.; Rubio-Bellido, C.; Canivell, J. Thermal Comfort in Social Housing in Ecuador: Do Free-Running Buildings Work in Current and Future Climates? *Buildings* **2025**, *15*, 2018. [CrossRef]
21. Molina, J.R.; Lefebvre, G.; Gómez, M.M. Study of the thermal comfort and the energy required to achieve it for housing modules in the environment of a high Andean rural area in Peru. *Energy Build.* **2023**, *281*, 112757. [CrossRef]
22. Mejia-Solis, E.; Arias, J.; Palm, B. Simple solutions for improving thermal comfort in huts in the highlands of Peru. *Heliyon* **2023**, *9*, e19709. [CrossRef] [PubMed]
23. Ragin, C.C. *Redesigning Social Inquiry: Fuzzy Sets and Beyond*; University of Chicago Press: Chicago, IL, USA, 2008. [CrossRef]
24. Cohen, J. *Statistical Power Analysis for the Behavioral Sciences*, 2nd ed.; Lawrence Erlbaum Associates: Hillsdale, NJ, USA, 1988.
25. Rihoux, B.; Ragin, C.C. (Eds.) *Configurational Comparative Methods: Qualitative Comparative Analysis (QCA) and Related Techniques*; Sage: Thousand Oaks, CA, USA, 2009. [CrossRef]
26. Dino, I.G.; Meral Akgül, C. Impact of climate change on the existing residential building stock in Turkey: An analysis on energy use, greenhouse gas emissions and occupant comfort. *Renew. Energy* **2019**, *141*, 828–846. [CrossRef]
27. Pessenlehner, W.; Mahdavi, A. Building morphology, transparence, and energy performance. In Proceedings of the Eighth International IBPSA Conference, Eindhoven, The Netherlands, 11–14 August 2003; pp. 1025–1032.
28. Rodrigues, E.; Amaral, A.R.; Rodrigues Gaspar, A.; Gomes, A. How reliable are geometry-based building indices as thermal performance indicators? *Energy Convers. Manag.* **2015**, *101*, 561–578. [CrossRef]
29. Lomas, K.J.; Ji, Y. Resilience of naturally ventilated buildings to climate change: Advanced natural ventilation and hospital wards. *Energy Build.* **2009**, *41*, 629–653. [CrossRef]

Disclaimer/Publisher's Note: The statements, opinions and data contained in all publications are solely those of the individual author(s) and contributor(s) and not of MDPI and/or the editor(s). MDPI and/or the editor(s) disclaim responsibility for any injury to people or property resulting from any ideas, methods, instructions or products referred to in the content.